

THE DIMINISHING IMPORTANCE OF MAJOR GALAXY MERGERS AT HIGHER REDSHIFTS

RIK J. WILLIAMS^{1,2}, RYAN F. QUADRI^{1,2,3}, MARIJN FRANX²

Accepted for publication in ApJ Letters

ABSTRACT

Using mass-selected galaxy samples from deep multiwavelength data we investigate the incidence of close galaxy pairs between $z = 0.4$ – 2 . Many such close pairs will eventually merge, and the pair fraction is therefore related to the merger rate. Over this redshift range the mean pair fraction is essentially constant (evolving as $f_{\text{pair}} \sim (1+z)^{-0.4 \pm 0.6}$) with about $6 \pm 1\%$ of massive galaxies having a $1:4$ or greater companion within $30h^{-1}$ kpc. Assuming the timescale over which pairs merge is not a strong function of redshift, this implies a similarly constant merger rate (per unit time) out to $z = 2$. Since about three times as much cosmic time passes at $z < 1$ as between $z = 1$ – 2 , this implies that correspondingly more mergers occur in the low-redshift universe. When minor companions ($1:10$ mass ratio or greater) are included, the pair fraction increases to $\sim 20\%$ and still does not evolve strongly with redshift. We also use a rest-frame color criterion to select pairs containing only quiescent galaxies (major “dry merger” progenitors), and find them to be similarly rare and constant with 4 – 7% of massive quiescent galaxies exhibiting a nearby companion. Thus, even though other studies find major mergers to be relatively uncommon since $z = 1$, our results suggest that few additional mergers occur in the $1 < z < 2$ range and other mechanisms may be required to explain the mass and size growth of galaxies over this epoch.

Subject headings: cosmology: observations — galaxies: evolution — galaxies: high-redshift — infrared: galaxies

1. INTRODUCTION

Most stellar mass in the universe was formed during a relatively brief chapter in its history, with the cosmic star-formation rate peaking around $z \sim 2$ (Lilly et al. 1996; Madau et al. 1996; Hopkins & Beacom 2006, and references therein). Cosmological models and simulations hold that local massive galaxies were hierarchically assembled, with massive $z = 0$ galaxies built from successive mergers of lower-mass constituents. Therefore, although many galaxies continue to add mass through star formation at lower redshifts, *assembly* processes (such as major mergers and satellite accretion) should play an increasingly important role at late times (Guo & White 2009). But recent observations reveal that the true picture is somewhat more nuanced: massive ($M_\star \gtrsim 10^{11} M_\odot$) galaxies, many of which have ceased significant star formation, exist at least up to $z \sim 2.5$ (Kriek et al. 2006, 2008b; Cassata et al. 2008; Stutz et al. 2008; Williams et al. 2009; Brammer et al. 2009, 2011). Although massive galaxies should continue growing through mergers, a substantial fraction of their mass was in place at $z = 2$.

Such hierarchical processes serve not only to build up the stellar masses of galaxies, but also affect their structural properties (e.g. effective radius, surface density, and mass profile) and morphologies. It now appears that most quiescent galaxies are extremely compact and dense for their mass at $z \sim 2.3$ (e.g. van Dokkum et al. 2008), but comparably dense objects are practically nonexistent in the local universe (Taylor et al. 2010). Moreover, the average size of quiescent galaxies increases (and surface density within the effective radius decreases) smoothly with time (e.g. Franx et al. 2008;

Damjanov et al. 2009; Williams et al. 2010). Gas-poor “dry mergers” have been proposed as a mechanism behind this growth, but the necessary evolution in the mass-size plane (much faster in size than mass) is difficult to achieve in equal-mass merging scenarios (Boylan-Kolchin et al. 2006). Several processes working in concert, including major mergers (e.g. Bell et al. 2006; Shankar et al. 2011), the quenching of progressively more extended star-forming galaxies at lower redshifts (van der Wel et al. 2009), and the accretion of stellar mass in the outskirts of these compact “cores” (due to minor mergers; Bezanson et al. 2009; Hopkins et al. 2009) may therefore drive this size evolution.

Mergers might thus play an important role in the buildup of massive galaxies, but observational determinations of their importance are still uncertain. At high redshifts mergers can be difficult to detect, though clues may nonetheless appear in galaxies’ morphologies (Conselice et al. 2003) and resolved velocity distributions (Förster Schreiber et al. 2009). Another promising technique is the use of close galaxy pairs as a proxy for mergers since these are easily detectable to high redshift and, on average, are expected to merge within a relatively short timescale (which can be calibrated using simulations; Bundy et al. 2009; Lin et al. 2011; Kitzbichler & White 2008, KW08).

Here we employ a deep 0.7 deg^2 multiwavelength survey to determine pair fractions between $z = 0.4$ – 2.0 . First we present a brief summary of the data used in this sample, then the method for deriving galaxy pair fractions and the conversion to merger rates, and finally we discuss the implications of the pair fraction evolution for galaxy formation. AB magnitudes and cosmological parameters $h = 0.7$, $\Omega_M = 0.3$, and $\Omega_\Lambda = 0.7$ are used throughout.

2. DATA AND DERIVED QUANTITIES

For this study we use a catalog (Williams et al. 2012, in preparation) compiled from the UKIDSS Ultra-Deep Survey

williams@obs.carnegiescience.edu

¹ Carnegie Observatories, 813 Santa Barbara St., Pasadena, CA 91101, USA

² Leiden Observatory, Leiden University

³ Hubble Fellow

(UDS; Lawrence et al. 2007; Warren et al. 2007) Data Release 8 and supplementary data. The datasets and techniques employed for generating this catalog are similar to those we used with the UDS DR1 in Williams et al. (2009); a brief summary follows. *Source Extractor* v2.5.0 (Bertin & Arnouts 1996) was run in dual-image mode to detect sources in the UDS DR8 K-band mosaic, measuring fluxes from a series of deep optical/NIR images: u' from archival CFHT data, $BVRi'z'$ from the Subaru-XMM Deep Survey (SXDS; Furusawa et al. 2008), and JHK from the UDS DR8, all convolved to the same point-spread function. Because of *Spitzer*'s much larger point-response function, we followed the deblending technique described by Labbé et al. (2006) and Wuyts et al. (2007) to extract matched $3.6\mu\text{m}$ and $4.5\mu\text{m}$ fluxes from deep *IRAC* imaging in the UDS field (SpUDS; PI J. Dunlop). Objects falling near bad pixels in the optical or near-IR images were excluded, as were those with no optical coverage, resulting in an effective image area of $\sim 0.7\text{deg}^2$.

From this updated catalog we calculate photometric redshifts with EAZY (Brammer et al. 2008), interpolate rest-frame colors with InterRest (Taylor et al. 2009), and derive galaxy masses with FAST (Kriek et al. 2009). The photometric redshifts agree to $\sim 2\%$ with spectroscopic redshifts in the field; most catastrophic outliers are efficiently removed via a χ^2 cut. In calculating the masses we assumed a Salpeter (1955) initial mass function (IMF), solar metallicity, and Bruzual & Charlot (2003) stellar population models, and applied a factor of -0.2dex to the masses to bring them in line with a Kroupa (2001) IMF (as in Franx et al. 2008; Williams et al. 2010). Although uncertainties on photometrically-derived quantities can be substantial, in IR-selected galaxy samples stellar masses and mass-to-light ratios are relatively robust (Kriek et al. 2008a; Muzzin et al. 2009). The catalog has a 95% point-source completeness limit of $K < 24.5$; following Marchesini et al. (2009), the corresponding *mass completeness* is estimated by scaling each galaxy to the mass it would have at a brighter $K = 24.0$ limit (to account for the fact that galaxies are not point sources); the 75th percentile of scaled galaxy masses thus provides an estimate of the 75% mass completeness limit, which we estimate as $\log M_* = 9.8$ at $z \sim 2$ for red galaxies ($U - V_{\text{rest}} > 1.5$).

3. PAIR FRACTION MEASUREMENTS

3.1. Major “wet” and “dry” merger candidates

We searched the catalog for pairs of galaxies with projected transverse separations $< 30h^{-1}$ proper kpc, mass ratios of 1 : 4 or greater, and require that the photometric redshifts of the galaxies in each pair lie within $|z_1 - z_2|/(1 + z_1) < 0.2$ (where the subscripts 1 and 2 refer to the more and less massive galaxy in each pair, hereafter denoted “primary” and “secondary” respectively). This large redshift separation ensures that few physically-associated pairs are missed (according to the analysis described in Quadri & Williams 2010). From inserting simulated pairs of point sources into the detection image, we find that SExtractor successfully deblends pairs with separations $\gtrsim 1''.2$; we thus exclude those with $< 13\text{kpc}$ separations (equivalent to $1''.5$ at $z \sim 2$, to account for extended galaxy profiles). Only pairs containing one primary galaxy above $M_1 > 3.2 \times 10^{10} M_\odot$ and a secondary within the 1 : 4 mass ratio constraint, i.e. $0.25 \leq M_2/M_1 < 1$, are counted. The constraints on M_1 and M_2/M_1 ensure that secondary galaxies are always above our $\log M_2 > 9.8$ completeness

limit for red galaxies at $z \sim 2$. Finally, the constituent galaxies within pairs are classified as either star-forming or quiescent based on the rest-frame color criteria of Williams et al. (2009); each pair thus represents a candidate “dry merger” (i.e. quiescent-quiescent galaxy pair) or “wet merger” (containing at least one star-forming galaxy).

Even with the relatively small angular separations and the requirement that galaxies within a pair be close in redshift, some apparent pairs are due to chance alignments. We correct for this by randomizing the positions of all galaxies over the survey area (while retaining the galaxies’ masses, redshifts, and quiescent/star-forming classifications), and re-running the pair-finding algorithm on this randomized catalog with the same selection parameters (see also Quadri & Williams 2010). This “mock catalog” process is repeated 20 times to reduce the uncertainty in the contamination rate, and the mean number of random pairs is subtracted from the total pair counts for each primary and secondary galaxy type.

These corrected pair fraction measurements are listed in Table 1 and shown in Figure 1. We define the pair fraction $f_{xy} = N_{xy}/N_x$ as the fraction of “primary” galaxies of type X which have a less-massive “secondary” companion of type y; e.g., f_{sq} is the fraction of $\log(M_*/M_\odot) > 10.5$ star-forming galaxies with quiescent galaxy companions (whose masses are $> 0.25M_{\text{primary}}$), counting each pair only once even if both members are above the primary mass threshold. The total pair fraction regardless of galaxy type, $f_{\text{all,all}}$, is also given. Assuming these pairs merge at some point in the future, this fraction is related to the number of merger *descendants* – i.e. how many mergers a massive $z = 0$ galaxy is likely to have undergone – as a function of redshift.

3.2. Mass dependence and minor pairs

While the pair sample in Table 1 makes full use of the galaxy catalog’s dynamic range, it is also instructive to consider higher-mass primary galaxies: both to determine whether the pair fraction depends on mass (e.g. Bundy et al. 2009; Bernardi et al. 2011), and to investigate lower-mass companions which may represent minor mergers. The procedure described above is therefore repeated for primary galaxies with $\log(M_*/M_\odot) > 10.8$ and companions within 1:4 and 1:10 mass ratios; these fractions are shown in Figure 2. Since star-forming galaxies are rare at this mass, only pairs with quiescent primary galaxies are included in this plot. Over all redshifts the 1:4 pair fractions are similar to those at $\log(M_*/M_\odot) > 10.5$ shown in Figure 1; this is not surprising, since these samples are not widely separated in mass and the uncertainties are large. Unfortunately, the dynamic range of the catalog does not allow a detailed analysis of mass dependence due to the relative rarity of very massive galaxies and the need to maintain a “secondary” sample above the survey completeness limit.

When minor companions are included, the pair fraction increases substantially: while only a few percent of these massive galaxies have a close neighboring galaxy of comparable mass, 15-20% have companions within a 1 : 10 ratio (Figure 2, bottom panel). Since high-mass galaxies are more likely to be quiescent, this increased pair fraction is largely due to star-forming companions; however, with the inclusion of lower-mass secondary galaxies there even appears to be a marginal increase in the “dry pair” fraction at each redshift. Although the “minor pair fraction” is substantially enhanced, this does not necessarily suggest a high minor merger rate since satellite mass and dynamical friction timescale are expected to be

inversely correlated (KW08).

3.3. Inferred merger timescales and rates

Galaxy pairs only represent merger *candidates*, as some apparent pairs will not coalesce even over many Gyr while others rapidly merge, depending on orbital properties, projection effects, and other internal factors. Thus, converting from pair fractions to merger rates requires an average timescale,

$$t_{\text{merg}} = N_{\text{pair}} / \dot{N}_{\text{merger}} \quad (1)$$

where N_{pair} is the number of close pairs within a given redshift bin and \dot{N}_{merger} is the number of mergers per unit time within the same galaxy population. One theoretical parametrization of this timescale was derived from the Millennium Simulation by KW08 as a function of galaxy mass, redshift, and maximum projected separation. Specifically, their formula for pairs with projected separations $\Delta r < 30h^{-1}$ kpc, $M_2/M_1 > 1/4$, and photometric redshifts gives a mean merger timescale of

$$\langle t_{\text{merg}} (h^{-1} \text{Myr}) \rangle^{-1/2} = 0.0189 - 9.47 \times 10^{-4} z + 6.71 \times 10^{-3} [\log(M_*/h^{-1} M_\odot) - 10] \quad (2)$$

In the KW08 formalism the same mass limit is imposed on both primary and secondary galaxies, while our sample includes lower-mass companions down to the survey limit. The resulting KW08 pair mass ratios depend on primary galaxy mass (i.e., closer to equal-mass near the survey limit). For consistency, we thus repeat the above exercise with their selection method. Two mass thresholds are applied: $\log(M_*/M_\odot) > 10.5$ as before, and $\log(M_*/M_\odot) > 10.0$ to take full advantage of the survey. These fractions, shown in the top panels of Figure 3, are somewhat lower than in Figure 1 where secondary galaxies below the primary mass threshold are included.

Figure 3 (bottom) shows the specific merger rates, calculated with eq. (2), from $z = 0.4 - 2$ at the two mass thresholds. Adopting the KW08 timescale, mergers are relatively rare: only about 0.5–1% of massive quiescent galaxies merge with quiescent companions each Gyr, and fewer than 10% of galaxies over this redshift range will undergo major mergers. This is due both to the rarity of massive galaxy pairs and to the long effective merger timescales from KW08, about 2–3.5 Gyr depending on mass and redshift. Although the KW08 formalism is most applicable to our specific pair selection parameters, a variety of timescales have been employed in the literature; this is discussed further in §4.1.

4. DISCUSSION

4.1. Connecting pairs to mergers

Close pairs of galaxies are easily identified and detectable to high redshift, and are therefore in principle a robust way of identifying systems that may merge within a relatively short timescale. But it is less straightforward to determine this timescale and convert the measured pair fractions to merger rates.

Several estimates of the merger timescale have been used in previous work. Bell et al. (2006) assume that galaxy pairs merge within roughly one orbital time, in their case ~ 0.4 Gyr, while the KW08 estimate is nearly an order of magnitude larger for the galaxy masses considered here. These fundamentally change the interpretation of the measured pair fractions: with the Bell et al. (2006) timescale, major mergers

play a significant role in the assembly of massive galaxies over time; assuming KW08, only about 20% of massive quiescent galaxies have undergone major mergers since $z = 2$, with $\sim 2/3$ of this occurring at $z < 1$. This disagreement is largely a result of the KW08 analysis including physically-associated galaxy pairs which are at relatively large real distances despite having close projected separations, and therefore merge only after a long period (or not at all). Nonetheless, if the merger timescale isn't a strong function of redshift, the unchanging pair fraction we measure reflects a similarly constant merger rate since $z = 2$.

4.2. Comparison to previous work

The pair fractions derived here are in broad agreement with previous work at $z \lesssim 1$. Bundy et al. (2009) find a low ($\sim 4\%$), non-evolving fraction of massive galaxies in “major pairs” at $z < 1.2$, with $10^{11} M_\odot$ galaxies more likely to have close companions than those with $10^{10} M_\odot$. Given their higher mass limit and smaller search radius ($20h^{-1}$ kpc), our $z < 1$ measurements appear to be in agreement: a total pair fraction of $\sim 4 - 8\%$, depending on whether the primary galaxies are star-forming or quiescent, and no strong evolution in the fraction. In addition, we confirm their reported higher incidence of “dry pairs” at lower redshifts, simply due to the coincident increase in the number density of massive quiescent galaxies. Between $0.4 < z < 0.8$, Bell et al. (2006) report a pair fraction of $5 \pm 1\%$ for galaxies above $2.5 \times 10^{10} M_\odot$, also in agreement with our pair fraction measurement at the same redshift.

One common theme in these studies is the rarity of dry mergers: even Bell et al. (2006), with their short assumed timescale, find that only $\sim 50\%$ of massive galaxies have undergone major mergers since $z = 0.8$; Bundy et al. (2009) estimate 30% at the high-mass ($10^{11} M_\odot$) end (but see Padilla et al. 2011). In their analysis of the environmental dependence of merger rate, Lin et al. (2011) estimate a somewhat higher rate in *high-density environments*: 1.2 ± 0.3 major dry mergers per galaxy since $z = 1$, perhaps not surprising since such environments harbor a larger fraction of quiescent galaxies (e.g. Kauffmann et al. 2004; Quadri et al. 2011). However, these only account for $38 \pm 10\%$ of the mass accretion of these galaxies. If the merging timescale doesn't vary strongly with redshift, our results suggest that the major merger rate at $1 < z < 2$ is comparable to that at $z < 1$; since twice as much cosmic time passes in the latter epoch than the former, this in turn implies that most major mergers occur below $z \sim 1$.

4.3. Major vs. minor mergers

Even when short timescales are assumed, dry mergers from $z = 2$ to the present occur perhaps once or twice per galaxy at most. Since strong size and mass growth are nonetheless seen over this same redshift interval (e.g. Franx et al. 2008; Williams et al. 2010), it appears that major mergers are *not* the primary driver behind the observed evolution. Indeed, if major dry mergers were the primary driver behind the smooth evolution in galaxy sizes and surface densities seen over $z = 0 - 2$, a much larger number would be required to eliminate the compact quiescent galaxy population by $z = 0$ (Taylor et al. 2010). Even if mergers are more common than the KW08 timescale implies, they still may not account for the evolution of the *mass-size* relation since major mergers increase galaxies' masses and sizes at similar rates.

Another explanation is that galaxies undergo many minor

mergers or accrete low-mass satellites. Naab et al. (2009) find that minor mergers are more efficient (per unit secondary galaxy mass) at increasing galaxy radii than major mergers. This accretion scenario is also attractive because it depends only weakly (if at all) on whether or not the central galaxy is forming stars, and might also partially explain the size growth observed in massive star-forming galaxies (Williams et al. 2010). As shown in Figure 2, the inclusion of minor companions increases the pair fraction to 15–20% (see also López-Sanjuan et al. 2011). However, the merging timescale of these minor galaxies is not well-understood: on one hand their dynamical friction timescales are longer than more massive satellites, but tidal effects may hasten the incorporation of minor satellites into a massive galaxy’s extended halo.

5. CONCLUSIONS

From deep mass-selected samples, we have performed the first analysis of major and minor galaxy pairs out to $z = 2$, distinguishing between “dry” and “wet” merger candidates. “Dry” pairs are relatively rare: only $\sim 3–7\%$ of massive quiescent galaxies have a quiescent companion of comparable mass (with an average companion mass 40% that of the

primary). This fraction increases slightly at lower redshifts, but the total pair fraction (including both star-forming and quiescent galaxies) remains essentially constant, evolving as $f_{\text{all,all}} \sim (1+z)^{-0.4 \pm 0.6}$. Minor companions are significantly more common, increasing to 15–20% for $> 1:10$ mass ratios. However, significant uncertainties remain when converting pair fractions to merger rates. Nonetheless, while galaxies are often assumed to assemble rapidly at high z , the constant pair fraction suggests that, in fact, massive galaxies undergo more mergers at $z < 1$ than $z = 1–2$. Unless the effective merger timescale is much shorter than the values assumed here, such mergers represent a rare and stochastic process that is unlikely to make more than a marginal contribution to the smooth mass and size growth seen since $z = 2$.

We thank the referee for helpful and constructive comments. R.J.W. acknowledges support from NSF grant AST-0707417. Much of this work was performed during working visits to Leiden, funded by the Netherlands Organization for Scientific Research (NWO) and the Leids Kerkoven-Bosscha Fonds.

REFERENCES

- Bell, E. F., et al. 2006, *ApJ*, 640, 241
 Bernardi, M., Roche, N., Shankar, F., & Sheth, R. K. 2011, *MNRAS*, 412, L6
 Bertin, E., & Arnouts, S. 1996, *A&AS*, 117, 393
 Bezanson, R., van Dokkum, P. G., Tal, T., Marchesini, D., Kriek, M., Franx, M., & Coppi, P. 2009, *ApJ*, 697, 1290
 Boylan-Kolchin, M., Ma, C.-P., & Quataert, E. 2006, *MNRAS*, 369, 1081
 Brammer, G. B., van Dokkum, P. G., & Coppi, P. 2008, *ApJ*, 686, 1503
 Brammer, G. B., et al. 2009, *ApJ*, 706, L173
 Brammer, G. B., et al. 2011, *ApJ*, In press (arXiv:1104.2595)
 Bruzual, G. & Charlot, S. 2003, *MNRAS*, 344, 1000
 Bundy, K., Fukugita, M., Ellis, R. S., Targett, T. A., Belli, S., & Kodama, T. 2009, *ApJ*, 697, 1369
 Cassata, P., et al. 2008, *A&A*, 483, L39
 Conselice, C. J., Bershad, M. A., Dickinson, M., & Papovich, C. 2003, *AJ*, 126, 1183
 Damjanov, I., et al. 2009, *ApJ*, 695, 101
 Förster Schreiber, N. M., et al. 2009, *ApJ*, 706, 1364
 Franx, M., van Dokkum, P. G., Förster Schreiber, N. M., Wuyts, S., Labbé, I., & Toft, S. 2008, *ApJ*, 688, 770
 Furusawa, H., et al. 2008, *ApJS*, 176, 1
 Guo, Q. & White, S. D. M. 2009, *MNRAS*, 396, 39
 Hopkins, A. M., & Beacom, J. F. 2006, *ApJ*, 651, 142
 Hopkins, P. F., Bundy, K., Murray, N., Quataert, E., Lauer, T., & Ma, C.-P. 2009, *MNRAS*, 398, 898
 Kauffmann, G., White, S. D. M., Heckman, T. M., Ménard, B., Brinchmann, J., Charlot, S., Tremonti, C., & Brinkmann, J. 2004, *MNRAS*, 353, 713
 Kitzbichler, M. G. & White, S. D. M. 2008, *MNRAS*, 391, 1489 (KW08)
 Kriek, M., et al. 2006, *ApJ*, 649, L71
 Kriek, M., et al. 2008a, *ApJ*, 677, 219
 Kriek, M., van der Wel, A., van Dokkum, P., Franx, M., & Illingworth, G. D. 2008b, *ApJ*, 682, 896
 Kriek, M., van Dokkum, P. G., Labbé, I., Franx, M., Illingworth, G. D., Marchesini, D., & Quadri, R. F. 2009, *ApJ*, 700, 221
 Kroupa, P. 2001, *MNRAS*, 322, 231
 Labbé, I., Bouwens, R., Illingworth, G. D., & Franx, M. 2006, *ApJ*, 649, L67
 Lawrence, A., et al. 2007, *MNRAS*, 379, 1599
 Lilly, S. J., Le Fevre, O., Hammer, F., & Crampton, D. 1996, *ApJ*, 460, L1
 Lin, L., et al. 2011, *ApJ*, 718, 1158
 López-Sanjuan, C., et al. 2011, *A&A*, 530, 20L
 Madau, P., Ferguson, H. C., Dickinson, M. E., Giavalisco, M., Steidel, C. C., & Fruchter, A. 1996, *MNRAS*, 283, 1388
 Marchesini, D., et al. 2009, *ApJ*, 701, 1765
 Muzzin, A., Marchesini, D., van Dokkum, P. G., Labbé, I., Kriek, M., & Franx, M. 2009, *ApJ*, 701, 1839
 Naab, T., Johansson, P. H., & Ostriker, J. P. 2009, *ApJ*, 699, L178
 Padilla, N., Christlein, D., Gawiser, E., & Marchesini, D. 2011, *A&A*, 531, 142
 Quadri, R. F., & Williams, R. J. 2010, *ApJ*, 725, 794
 Quadri, R. F., Williams, R. J., Franx, M., & Hildebrandt, H. 2011, *ApJ*, Submitted (arXiv:1104.1426)
 Salpeter, E. E. 1955, *ApJ*, 121, 161
 Shankar, F., Marulli, F., Bernardi, M., Mei, S., Meert, A., & Vikram, V. 2011, *MNRAS*, Submitted (arXiv:1105.6043)
 Stutz, A. M., Papovich, C., & Eisenstein, D. J. 2008, *ApJ*, 677, 828
 Taylor, E. N., et al. 2009, *ApJ*, 694, 1171
 Taylor, E. N., Franx, M., Glazebrook, K., Brinchmann, J., van der Wel, A., & van Dokkum, P. 2010, *ApJ*, 720, 723
 van der Wel, A., Bell, E. F., van den Bosch, F. C., Gallazzi, A., & Rix, H.-W. 2009, *ApJ*, 698, 1232
 van Dokkum, P. G., et al. 2008, *ApJ*, 677, L5
 Warren, S. J., et al. 2007, *MNRAS*, 375, 213
 Williams, R. J., Quadri, R. F., Franx, M., van Dokkum, P., & Labbé, I. 2009, *ApJ*, 691, 1879
 Williams, R. J., Quadri, R. F., Franx, M., van Dokkum, P., Toft, S., Kriek, M., & Labbé, I. 2010, *ApJ*, 713, 738
 Wuyts, S., et al. 2007, *ApJ*, 655, 51

TABLE 1
PAIR FRACTIONS IN THE UKIDSS-UDS

z_{phot}	N_Q	N_S	f_{Qq}	f_{Qs}	f_{Sq}	f_{Ss}	$f_{\text{all,all}}$
$0.4 < z < 0.8$	270	77	0.066 ± 0.017	0.013 ± 0.009	0.035 ± 0.026	-0.001 ± 0.013	0.069 ± 0.016
$0.8 < z < 1.2$	495	163	0.046 ± 0.011	0.016 ± 0.008	0.046 ± 0.019	0.015 ± 0.014	0.062 ± 0.012
$1.2 < z < 1.6$	692	292	0.053 ± 0.010	0.020 ± 0.007	0.037 ± 0.014	-0.001 ± 0.008	0.062 ± 0.010
$1.6 < z < 2.0$	376	387	0.031 ± 0.011	0.040 ± 0.012	0.011 ± 0.008	0.025 ± 0.010	0.054 ± 0.010

NOTE. — Uppercase subscripts denote the “primary” galaxy type: quiescent (Q) or star-forming (S); lowercase denote the type of the secondary galaxy within a pair. Hence “ f_{Qs} ” is the fraction of massive quiescent galaxies with a star-forming companion. Here all primary galaxies have masses above $\log M_1 > 10.5$, secondaries are above $\log M_2 > 9.9$, and a mass ratio constraint of $0.25 < M_2/M_1 < 1$ has been imposed.

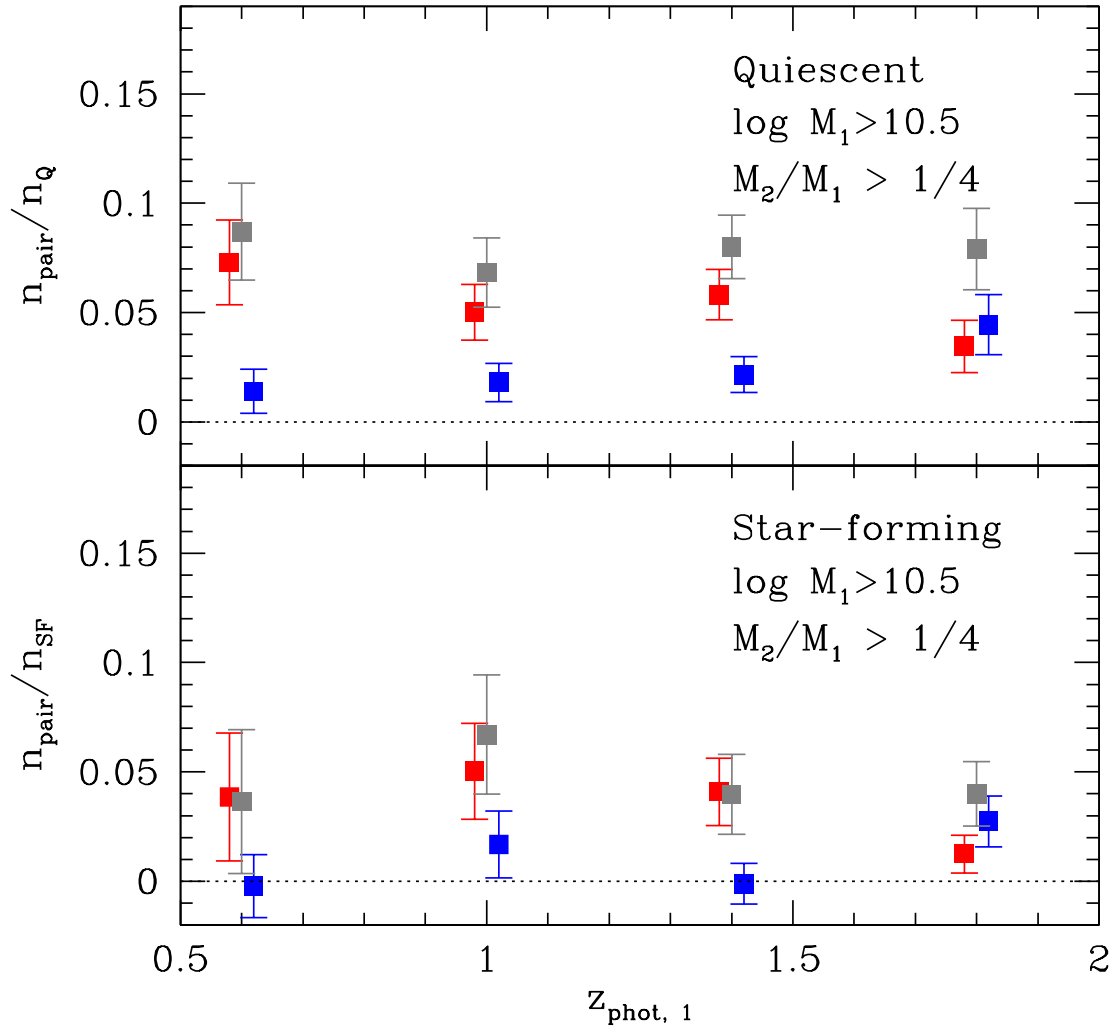


FIG. 1.— Evolution of the massive galaxy pair fraction, defined as the fraction of massive “primary” galaxies ($\log(M_1/M_\odot) > 10.5$) which have close companions within a 1:4 mass ratio (i.e. $0.25 \leq M_2/M_1 < 1$; the average mass ratio is $M_2/M_1 \sim 0.4$). The top and bottom panels show this fraction for quiescent and star-forming primary galaxies respectively. Red, blue, and grey points denote the fractions of quiescent, star-forming, and total *secondary* galaxies, respectively; thus, the red points in the top panel show the prevalence of major “dry merger” progenitors. The total pair fraction is remarkably constant over this redshift range.

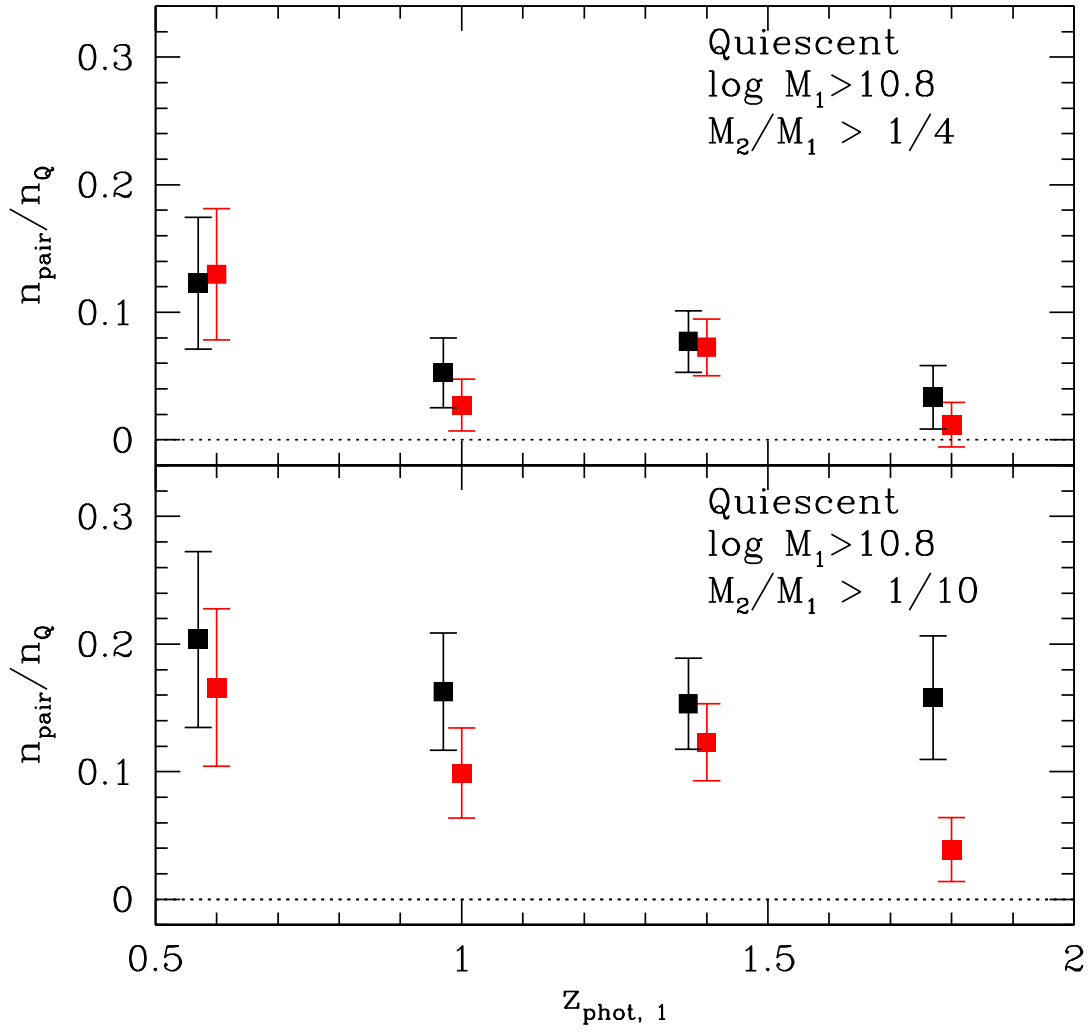


FIG. 2.— Comparison of pair fractions with two different mass ratios ($M_2/M_1 > 1/4$ and $M_2/M_1 > 1/10$) as a function of redshift. Here all “primary” galaxies are quiescent and 0.3 dex higher in mass than in Figure 1; black points show the fraction of primary galaxies with any close companions within the given mass ratio, while red points denote quiescent secondary galaxies (“dry mergers”) only. In both mass ranges the pair fraction is constant or weakly declining with redshift.

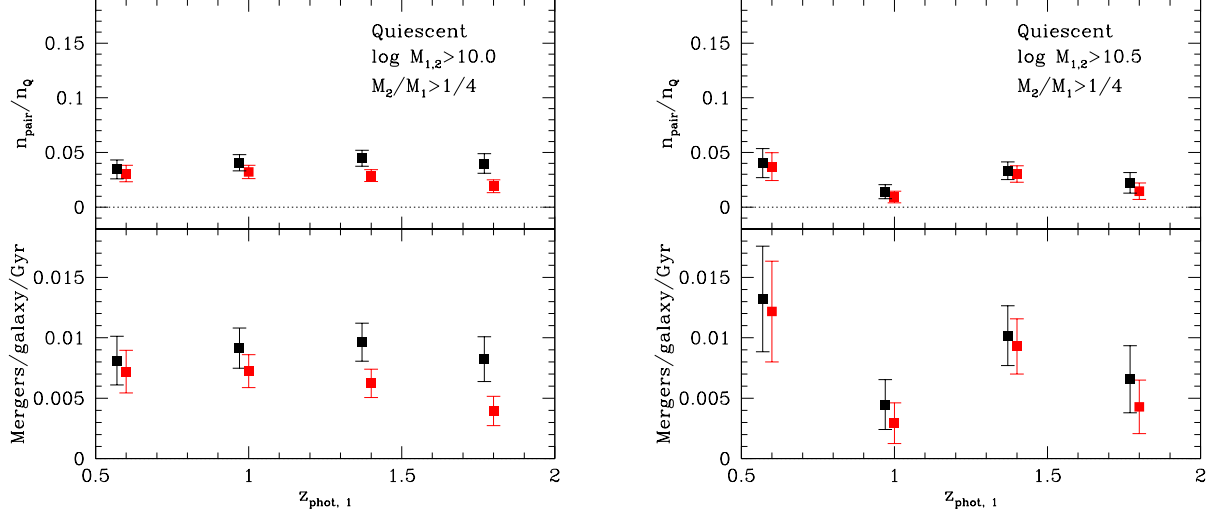


FIG. 3.— Top panels: Pair fractions of quiescent primary galaxies determined using the same mass threshold for both primary and secondary galaxies. This is the selection method used in the theoretical merger timescale calibration developed by KW08. Bottom panels: Merger rates computed from the measured pair fractions and KW08 timescales. In all panels, red points denote quiescent-quiescent galaxy pairs (“dry mergers”) while black points include both star-forming and quiescent secondary galaxies. The left and right panels show the same calculation for mass limits of $\log M_{\star}/M_{\odot} = 10.0$ and 10.5 respectively. Note the fractions in the right panel differ from Figure 1 due to the higher mass limit imposed on the secondary galaxies; in both cases the inferred merger rates are essentially constant and quite low.